APPENDIX A

Numbers of Acorns

Estimates of acorn production were made in years 2012 through 2020 by measuring during the middle of October the mass of acorns in a one square meter plot under each of six oak trees within the study area. The same trees and the same plots were used each year for estimation of acorn production to assess variability among years and relationship to changes in abundance of the tree squirrels. The data appear in Table A1.

Table A1. Mass of acorns (g) in a 1 m^2 plot under each tree in the study area.

	Year								
Tree	2012	2013	2014	2015	2016	2017	2018	2019	2020
Blue Oak	0	250	6	83	0	7	12	0	98
Canyon Oak	230	960	0	53	54	19	27	84	68
Coast Live Oak	18	290	18	29	3	5	3	0	5
Coast Live Oak	75	880	6	0	2	4	0	1	16
Coast Live Oak	69	590	2	34	39	4	0	0	24
Coast Live Oak	2	680	2	10	14	0	0	0	136
Mean ± s.e.	65.7 ± 35.5	608.3 ± 120.1	5.7 ± 2.7	34.8 ± 12.3	18.7 ± 9.2	6.5 ± 2.7	7.0 ± 4.4	14.2 ± 14.0	57.8 ± 21.2

APPENDIX B

Numbers of Juvenile and Subadult Squirrels

Starting in January 2015, observers at our field site started distinguishing among adults, subadults, and juveniles. The latter two categories can serve as a proxy for reproduction. Figure A1 shows the numbers of juveniles and subadults for the WGS and the FS. For both species, juveniles and subadults are seen more often in spring and fall (Fig. A1, shaded areas), especially in the case of the FS. However, there is a great deal of year-to-year variation (long timescales) in the numbers.

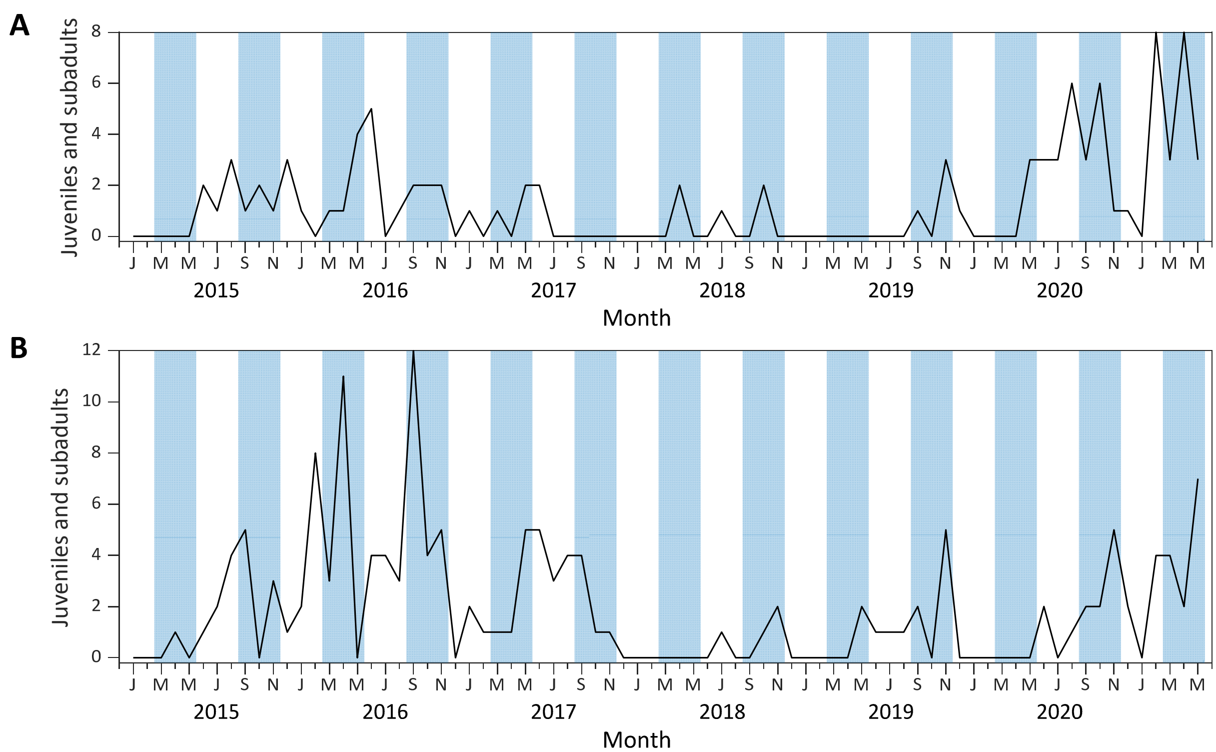

Figure A1. Monthly time series for numbers of juveniles and subadults for (A) the WGS and (B) the FS from January 2015 through May 2021. The shaded regions represent spring (March-May) and fall (September-November).

APPENDIX C

Annual and Semiannual Temperature Cycles

Meteorologists and climatologists have used harmonic analysis to identify seasonal cycles in atmospheric temperature (White & Wallace 1978). In addition to a strong annual cycle, a semi-annual cycle, which can vary by year and location, has been identified (White & Wallace 1978; North *et al.* 2021). In their equation (1), North *et al.* (2021) used the first two terms of a Fourier representation of an annual temperature times series. Their equation, using months as the time unit, is given by

$$x_t = a_0 + A_1 \cos\left(\frac{2\pi(t+\phi_1)}{12}\right) + A_2 \cos\left(\frac{4\pi(t+\phi_2)}{12}\right), \qquad \text{(A1)}$$

Where x_t is the temperature (in °C), t is the time (in months), a_0 is the center value for the temperature oscillations (in °C), A_i is the amplitude (in °C) and ϕ_i is the phase shift (in months) of the annual (i=1) and semi-annual (i=2) component cycles.

We fit equation (A1) to the mean monthly temperature data from Ontario Airport (ONT) (Fig. 4a) using the method of nonlinear least squares. The parameter estimates and their standard errors appear in Table A2. The phase shifts are relative to the month of September. The temperature data and the fitted function appear in Fig. A2. The fitted function provides a good description of the observed temperature time series.

Figure A2 also shows, separately, the two component cycles. The annual cycle is the larger of the two and is obtained by setting $A_2 = 0$ in equation (A1). It peaks in July-August and has its trough in January-February. The smaller semi-annual cycle, obtained by setting $A_1 = 0$ in equation (A1), peaks twice per year in February-March and August-September and has its troughs in November-December and May-June. The amplitude of the semi-annual cycle is 21% the size of the amplitude of the annual cycle.

We fit equation (A1) to the observed temperature time series with $A_2 = 0$, so that only the annual cycle was present. The parameter estimates and their standard errors are also presented in Table A2. We computed the following Akaike Information Criterion (AIC) for both fitted models:

$$AIC = n \ln\left(\frac{SS_E}{n}\right) + 2k ,$$

where $n = 140$ is the sample size, SS_E is the residual sum of squares for the regression, and k is the number of fitted parameters ($k = 3$ for the annual model and $k = 5$ for the model with both annual and semi-annual cycles). The annual model had an AIC of 165.02 and the model with both annual and semi-annual cycles had an AIC of 114.82. The smaller AIC suggests that the model with both cyclic components is a better description of the seasonal temperature changes. The magnitude of the difference, ΔAIC = 50.20, suggests that the annual model has little support relative to the full model.

Table A2. Parameter estimates and standard errors for full and annual models.

Parameter	Description	Estimate (± SE) for Full Model	Estimate (± SE) for Annual Model
a_0	center value of cycles (°C)	19.50 ± 0.12	19.49 ± 0.15
A_1	amplitude of annual cycle (°C)	6.82 ± 0.18	6.80 ± 0.21
ϕ_1	phase of annual cycle (mo.)	1.52 ± 0.05	1.53 ± 0.06
A_2	amplitude of semi-annual cycle (°C)	1.42 ± 0.18	—
ϕ_2	phase shift of semi-annual cycle (mo.)	0.48 ± 0.12	—

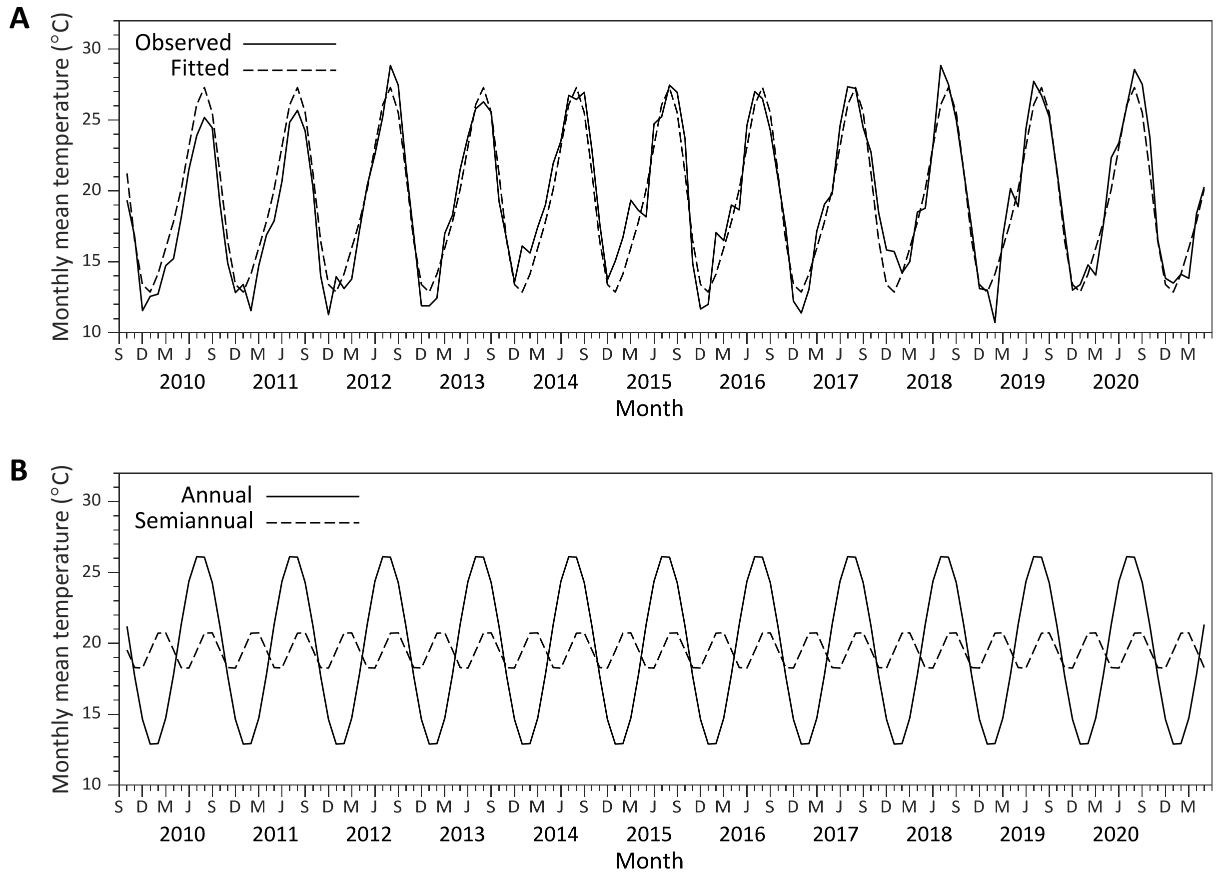

Figure A2. (A) Time series for observed and fitted mean monthly temperatures from Ontario Airport. (B) Plots of the component annual and semiannual cycles from the full model (C1).

APPENDIX D

Mean Annual Temperature Data for Ontario Airport

We conducted a spectral analysis of mean annual temperatures for Ontario Airport (ONT). The data values are the averages of the 12 mean monthly temperatures for each year. The first year of complete data is for 1999, so the time series spans 22 years from 1999 through 2021 (Fig. A3, panel A). We used the same methods as described section in section 2.5 for climate data: we detrended the data by fitting a quadratic polynomial using least squares, computed the standardized residuals, and computed a smoothed normalized spectrum for the residual time series. Because the time series is relatively short, we used smaller spans of 3 and 3 data points for the two iterations of the smoothing algorithm. We computed 95% significance thresholds by generating 2000 random permutations of the residuals, obtaining a smoothed normalized spectrum for each, and using the 2.5th and 97.5th percentiles of these surrogate spectra for the 95% limits.

Figure A3 shows the ONT temperature data and spectrum. The fitted quadratic polynomial (dashed line in Fig. A3, panel A) is nearly linear and suggests a trend of increasing temperatures. Although the significance band is wide due to the short length of the time series, the spectrum for the residuals shows a significant peak at a timescale of about 7 years (Fig. A3, panel B). This corresponds to the timescale range of the local peak in mean wavelet power in the lower right corner of Fig. 8.

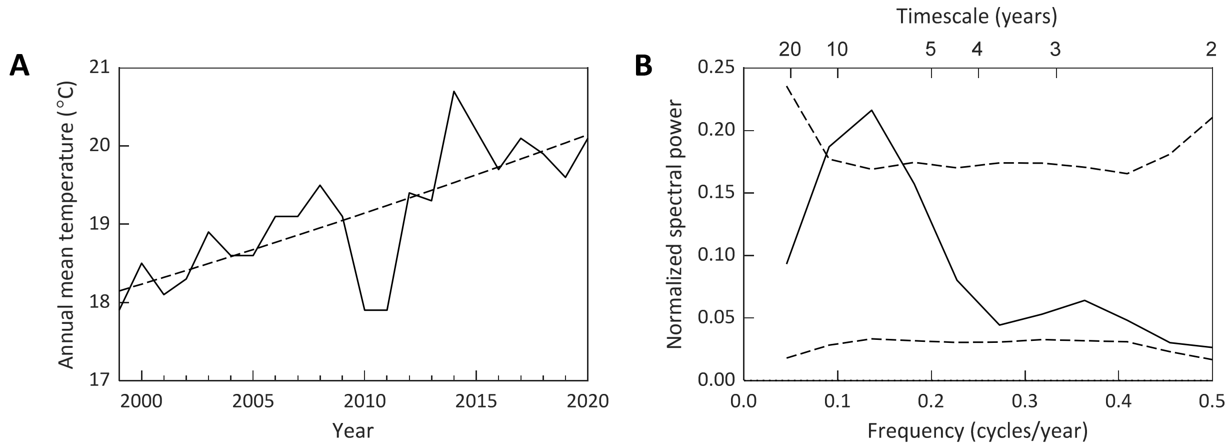

Figure A3. (A) Time series for observed mean annual temperatures from Ontario Airport. The dashed line is the fitted quadratic trend curve which is nearly linear. (B) Smoothed normalized spectrum for the standardized residuals from the temperature time series in panel A. Dashed lines are 95% significance thresholds for the null hypothesis of no timescale dependence in the ordering of the residuals.